SPECIAL SESIONS

Applications of Computer Algebra - ACA2018

June 18–22, 2018

Santiago de Compostela, Spain

S2

Computer Algebra Modeling in Science and Engineering

Thursday

Thu 21st, 10:00 - 10:30, Aula 7 – Ryszard Kozera:
Leap-Frog Algorithm for interpolating reduced sparse data

Thu 21st, 10:30 - 11:00, Aula 7 – Ryszard Kozera:
Reparameterization and piecewise cubics for interpolating reduced data

Thu 21st, 11:30 - 12:00, Aula 7 – Satoshi Yamashita:
Visualization of Planetary Motions Using KeTCindy

Thu 21st, 12:00 - 12:30, Aula 7 – Mukhtar Minglibayev:
Computing Perturbations in Two-Planetary Three-Body Problem with Masses Varying Non-Isotropically at Different Rates

Thu 21st, 12:30 - 13:00, Aula 7 – Alexander Prokopenya:
Motion of two bodies coupled by a spring on a rough plane with variable coefficient of friction: simulation with Mathematica

Thu 21st, 16:30 - 17:00, Aula 7 – Haiduke Sarafian:
A study of sensitivity of nonlinear oscillations of a CLD parallel circuit to parametrization of Esaki diode

Thu 21st, 17:30 - 18:00, Aula 7 – Hassane Djebouri:
Numerical study of multiphase flow and viscous fingering in a heterogeneous porous medium

Thu 21st, 18:00 - 18:30, Aula 7 – Kamel Touahir:
3D Stress analysis of a loaded birefringent sphere by photoelastic experiment and finite elements method

Thu 21st, 18:30 - 19:00, Aula 7 – Salah Zouaoui:
Fluid/Particles Flow Simulation by Finite Volume Method –Hybrid Approach

Organizers

Alexander Prokopenya:
Faculty of Applied Informatics and Mathematics,
Warsaw University of Life Sciences – SGGW, Poland

Haiduke Sarafian:
Professor of Physics and Endowed Chair of John T. and Paige S. Smith Professor of Science,
The Pennsylvania State University, USA

Aim and scope

The progressive impact of the Computer Algebra Systems (CAS) in science-based disciplines vividly is noticeable. It is rare to encounter a scientific investigation that is immune from its beneficial influences. Symbolic capabilities of the CAS provides forum to perform amazing calculations that practically are impossible otherwise. Within the last 25 years, applications of the CAS are extended beyond the peculiarities of scientific disciplines such as: biology, chemistry, microbiology, and physics, and has become the tool of the choice for analyzing engineering and mathematical challenging problems. For instance, dynamic simulations of engineering issues are addressed and mathematical conjectures are formulated and verified. Applications of the CAS lend it beyond the researchers' tools and have become powerful pedagogical instruments. The latter is suitable to engage the computer savvy generation promoting the discipline of interest.

The purpose of organizing this session is to bring together enthusiastic users of the Computer Algebra Systems in science, engineering and mathematics. Expected topics of presentations include (but are not limited to):

- Symbolic and numerical methods solving ODEs
- Modeling and simulation in physics
- Simulation of quantum computation
- Perturbation theories
- Stability and motion control
- Applications in biology, chemistry, and microbiology
- Modeling in finance and economics

Applications of Computer Algebra – ACA2018
Santiago de Compostela, June 18–22, 2018

Numerical study of multiphase flow and viscous fingering in a heterogeneous porous medium

Hassane DJEBOURI[1], **Salah ZOUAOUI**[1], **Kamal MOHAMMEDI**[2] and **Ali BILEK**[1]

This work deals with the numerical study of an immiscible water-oil displacement through a porous medium. This type of flow finds its application in many industrial processes [1]. The purpose of this work is to see the effect of the heterogeneity of the porous medium on the instability of the interface of the two fluids. This instability develops by the formation of viscous fingering at the interface [2].
The first work on this phenomenon began in the fifties (1951), but it still remains a topic of interest for many researchers [2]. In order to investigate the effect of the heterogeneity of the medium on this phenomenon, four cases are considered: the first one is a reference case where the porous medium is homogeneous. For the second and the third case, the medium is composed of two zones of the same porosity but of different permeability. The ratio of permeability between the two zones is equal to 1/3. In the second case, the injection is made in the zone that has the higher permeability and inversely in the third case.
In the last case we are interested in a fractured porous medium. The fracture has an opening of 2cm located in the middle of the domain (see figure 1).

Mathematical model

The studied domain is two-dimensional $\Omega \in R^2$. The mass conservation equations supplemented by Darcy's law allows to write [3]:

$$\frac{\partial(\phi.\rho_i.S_i)}{\partial t} - \nabla.\left(\rho_i \frac{\mathrm{K}.K_{ri}}{\mu_i}(\nabla P_i)\right) = 0 \qquad i = oil, water \tag{1}$$

Where ϕ and K are respectively the porosity and the permeability of the porous medium. K_{ri}, S_i, ρ_i and μ_i are respectively the relative permeability, the saturation, the density and the viscosity of the i phase.
This system of equations is completed by the following relations:

$$S_o - S_w = 1 \tag{2}$$

$$K_{ri} = K_{ri}(S_{ri}) \tag{3}$$

$$P_c = P_o - P_w \tag{4}$$

The Corey and CSF (Continuum Surface Force) models are used to calculate relative permeability and capillary pressure, respectively.
The initial conditions as well as the boundary conditions are:

- At $t = 0$, the medium is completely saturated with oil then: $S_o = 1$.
- The boundaries of the domain are impervious: $\frac{\partial S_i}{\partial n} = 0$ et $\frac{\partial P_i}{\partial n} = 0$.
- Injection and production point pressures are $1.79MPa$ and $1.31MPa$.

Figure 1: Different porous media studied

Table 1: Physical properties of porous media

	midium1	midium2		midium3		midium4	
Porosity (%)	30	Zone1	Zone2	Zone1	Zone2	Zone1	Zone2
		30	30	30	30	30	30
Absolute Permébility (m^2)	$130x10^{-12}$	$130x10^{-12}$	$43.33x10^{-12}$	$43.33x10^{-12}$	$43.33x10^{-12}$	$130x10^{-12}$	$130x10^{-12}$

Résultats

The finite volume method is used to solve this problem. Some results are presented:

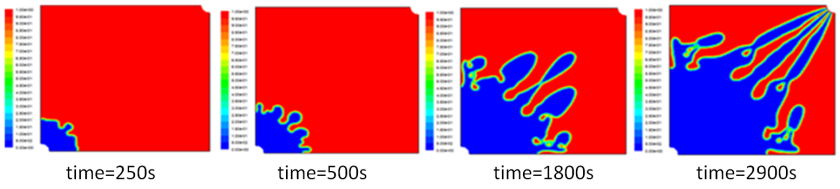

Figure 2: Displacement fronts and fingering patterns for medium1 at different times

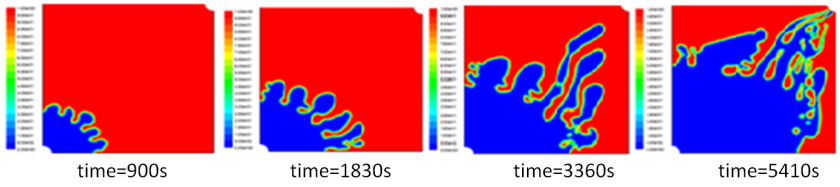

Figure 3: Displacement fronts and fingering patterns for medium2 at different times

The following observations are made:

- The characteristics of the porous medium modify the behavior of the water-oil interface and the appearance of breakthrough. This result is in agreement with previous studies.
- Viscous fingers tend to develop almost linearly according to the square root of time. These observations are in contradiction with the results of (Milad

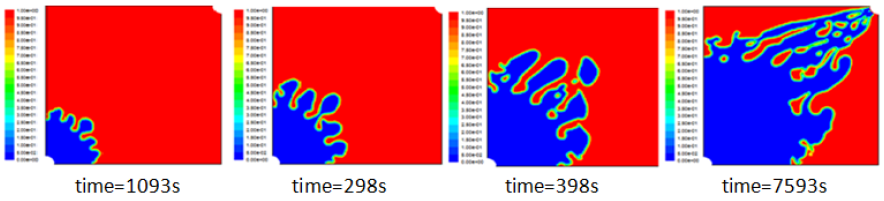

Figure 4: Displacement fronts and fingering patterns for medium3 at different times

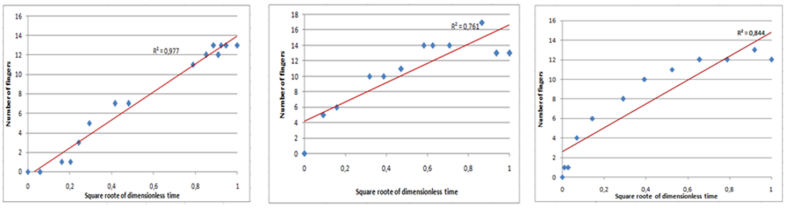

Figure 5: Number of fingers formed as a function of the square root of the dimensionless time for media 1, 2 and 3

Arabloo et al, 2015) but in good agreement with the experimental results of de (Yadali Jamaloei et al, 2010) and (Shokrollahi et al, 2013).

Keywords: heterogeneous porous media, multiphase flow, viscous fingering, fracture

References

[1] MILAD ARABLOO ET AL., Characterization of viscous fingering during displacements of low tension natural surfactant in fractured multi-layered heavy oil systems. *Chemical Engineering Research and Design* **96**, 23–34 (2015).

[2] R. FARAJZADEH ET AL., Simulation of instabilities and fingering in surfactant alternating gas (SAG) foam enhanced oil recovery. *Journal of Natural Gas Science and Engineering, JNGSE* **34**, 1191–1204 (2016).

[3] T. SHEORY ET AL., Numerical experiments in the simulation of enhanced oil recovery. *Internat.J. Thermal Sci.* **40**(11), 981–997 (2001).

[1]LMSE Laboratory, Mechanical Engineering Department
Mouloud Mammeri University of Tizi-Ouzou
P.O. Box17 RP, 15000 Tizi Ouzou, Algeria
zouaoui_salah2003@yahoo.fr; zouaouisalah@ummto.dz

[2]Unité de Recherche Matériaux, Procédés et Environnement (URMPE)
MESOnexusteam
Université M'hamed Bougara Boumerdès
Algérie 35000
mohammedik@yahoo.com

Applications of Computer Algebra – ACA2018
Santiago de Compostela, June 18–22, 2018

Leap-Frog Algorithm for interpolating reduced sparse data

Ryszard Kozera[1,2,3], **Lyle Noakes**[3]

We discuss the problem of fitting *ordered data points* $\mathcal{M} = \{x_i\}_{i=0}^n$ (with $n \geq 2$) from arbitrary Euclidean space E^m. The class $\mathcal{I}_T$ of piecewise C^2 interpolants $\gamma : [0, T] \rightarrow E^m$ (where $0 < T < \infty$) to interpolate reduced data $\mathcal{M}$ admits *free knots* $\mathcal{T} = \{t_i\}_{i=0}^n$ satisfying $\gamma(t_i) = x_i$ (here $t_0 = 0$ and $t_n = T$ are fixed). More precisely, it is assumed here that any choice of ordered interpolation knots $\{t_i\}_{i=0}^n$ together with $\mathcal{M}$ generates a curve $\gamma \in C^1([0, T])$ which is also C^2 over each subsegment (t_i, t_{i+1}) (where $i = 0, 1, \ldots, n-1$). A standard result (see [1] or [2]) claims that for given fixed knots $\{t_i\}_{i=0}^n$ the *optimal* curve $\gamma_{opt} \in \mathcal{I}_T$ to minimize:

$$\mathcal{J}_T(\gamma) = \sum_{i=0}^{n-1} \int_{t_i}^{t_{i+1}} \|\ddot{\gamma}(t)\|^2 dt \ , \tag{1}$$

coincides with the unique natural cubic spline $\gamma_{opt} = \gamma_{NS}$. Thus upon relaxing the unknown knots $\{t_i\}_{i=1}^{n-1}$, optimizing (1) over $\mathcal{I}_T$ reduces into a respective search over the class of natural splines, clearly contained in $\mathcal{I}_T$. Consequently, as each γ_{NS} is uniquely determined by data points $\mathcal{M}$ and the respective knots $\mathcal{T}$ (see [1]) the above infinite dimensional optimization task forms a finite dimensional one. Indeed, as recently shown (see [3]) for given $\mathcal{M}$, the task of minimizing (1) over $\mathcal{I}_T$ reformulates into optimizing the corresponding J_0 this time depending merely on $(t_1, t_2, \ldots, t_{n-1})$ variables, subject to $t_0 = 0 < t_1 < ... < t_n = T$. The latter constitutes a highly non-linear optimization task depending on $n-2$ variables. The application of standard numerical schemes to optimize J_0 often results in computational difficulties. In this work we adapt *a Leap-Frog scheme* (see e.g. [4]) to numerically optimize J_0. In our setting, this iterative scheme relies on the overlapped local optimizations each time depending on one variable only. The symbolic calculations performed with the aid of *Mathematica* software package (see e.g. [5]) permit to derive the corresponding local optimization schemes and to address the unimodality issue. Finally, the numerical tests comparing Leap-Frog scheme against Newton's or Secant methods are also carried out.

Keywords: Interpolation, reduced data, optimization.

References

[1] C. DE BOOR, *A Practical Guide to Spline*. Springer-Verlag, New York Heidelberg Berlin, 1985.

[2] B.I. KVASOV, *Methods of Shape-Preserving Spline Approximation*. World Scientific Publishing Company, Singapore, 2000.

[3] R. KOZERA; L. NOAKES, Non-linearity and non-convexity in optimal knots selection for sparse reduced data. *Computer Algebra in Scientific Computing*, *Lecture Notes in Computer Science*, Springer, **10490**, 257–271 (2017).

[4] R. KOZERA; L. NOAKES, Nonlinearities and noise reduction in 3-source photometric stereo. *Journal of Mathematical Imaging and Vision* **18**(2), 119–127 (2003).

[5] S. WOLFRAM, *The Mathematica Book*. Wolfram Media, 2003.

[1]Faculty of Applied Informatics and Mathematics
Warsaw University of Life Sciences - SGGW
Nowoursynowska str. 159, 02-776 Warsaw, Poland
ryszard.kozera@gmail.com

[2]Faculty of Mathematics, Informatics and Landscape Architecture
The John Paul II Catholic University of Lublin
Konstantynów str. 1 H, 20-708 Lublin, Poland

[3]School of Computer Science and Software Engineering
The University of Western Australia
Stirling Highway 35, Crawley, Perth, WA 6009, Australia

[4]School of Mathematics and Statistics
The University of Western Australia
Stirling Highway 35, Crawley, Perth, WA 6009, Australia
lyle.noakes@uwa.edu.au

Applications of Computer Algebra – ACA2018
Santiago de Compostela, June 18–22, 2018

Reparameterization and piecewise cubics for interpolating reduced data

Ryszard Kozera[1,2,3], **Magdalena Wilkołazka**[3]

We discuss the problem of estimating the unknown regular curve $\gamma : [0,T] \to E^n$ based on the so-called *reduced data* Q_m. The latter represent $m+1$ ordered interpolation points $Q_m = \{q_i\}_{i=0}^m$ in arbitrary Euclidean space E^n satisfying $q_i = \gamma(t_i)$. Here the respective knots $\mathcal{T}_m = \{t_i\}_{i=0}^m$ fulfilling $t_i < t_{i+1}$ are not given. In order to fit Q_m with any interpolation scheme (see e.g. [1]), the missing knots $\mathcal{T}_m$ must be replaced somehow with $\hat{\mathcal{T}}_m = \{\hat{t}_i\}_{i=0}^m$ subject to $\hat{t}_i < \hat{t}_{i+1}$. One of the possible choices is the so-called *exponential parameterization* depending on a single parameter $\lambda \in [0,1]$ and Q_m - see e.g. [2]. Note that $\lambda = 1$ renders a well-know *cumulative chord parameteriztion*. Different interpolation schemes are studied to fit reduced data Q_m - see e.g. [3], [4] or [5].

Recent work [6] and [7] addresses the issue of interpolating Q_m based on exponential parameterization applied to either modified Hermite interpolants $\hat{\gamma}_H \in C^1$ or to piecewise C^1 Lagrange cubics $\hat{\gamma}_C$. It is proved that for $\hat{\gamma} = \gamma_H$ or $\hat{\gamma} = \hat{\gamma}_C$ the following asymptotics in $\gamma \in C^4$ estimation holds (uniformly over $[0,T]$):

$$(\hat{\gamma}\circ\psi)(t) = \gamma(t) + O(\delta_m^1) \text{ for } \lambda \in [0,1) \text{ and } (\hat{\gamma}\circ\psi)(t) = \gamma(t) + O(\delta_m^4) \text{ for } \lambda = 1. \tag{1}$$

Here the mapping $\psi : [0,T] \to [0,\hat{T}]$ for each $\hat{\gamma}$ is specifically constructed. In this work we formulate and prove (with the aid of *Mathematica* package [8]) sufficient conditions for ψ to be a genuine reparameterization. Geometrical and algebraic insight is also given. Finally, with the aid of symbolic and analytic calculation sharpness of (1) is verified and justified.

Keywords: Interpolation, reduced data, convergence, sharpness and parameterization.

References

[1] C. DE BOOR, *A Practical Guide to Spline*. Springer-Verlag, New York Heidelberg Berlin, 1985.

[2] B.I. KVASOV, *Methods of Shape-Preserving Spline Approximation*. World Scientific Publishing Company, Singapore, 2000.

[3] R. KOZERA, Curve modeling via interpolation based on multidimensional reduced data. *Studia Informatica* **4B**(61), 1–140 (2004).

[4] R. KOZERA; L. NOAKES, Piecewise-quadratics and ε-uniformly sampled reduced data. *Applied Mathematics and Information Sciences* **10**(1), 33–48 (2016).

[5] R. KOZERA; L. NOAKES, C^1 interpolation with cumulative chord cubics. *Fundamenta Informaticae* **61**(3-4), 285–301 (2004).

[6] R. KOZERA; M. WILKOŁAZKA, Convergence order in trajectory estimation by piecewise-cubic and exponential parameterization. *Mathematical Modelling and Analysis*, submitted.

[7] R. KOZERA; M. WILKOŁAZKA, Modified Hermite interpolation with exponential parameterization. *Mathematics in Computer Science*, submitted.

[8] S. WOLFRAM, *The Mathematica Book*. Wolfram Media, 2003.

[1]Faculty of Applied Informatics and Mathematics
Warsaw University of Life Sciences - SGGW
Nowoursynowska str. 159, 02-776 Warsaw, Poland
ryszard.kozera@gmail.com

[2]School of Computer Science and Software Engineering
The University of Western Australia
Stirling Highway 35, Crawley, Perth, WA 6009, Australia

[3]Faculty of Mathematics, Informatics and Landscape Architecture
The John Paul II Catholic University of Lublin
Konstantynów str. 1 H, 20-708 Lublin, Poland
magda.wilkolazka@gmail.com

Applications of Computer Algebra – ACA2018
Santiago de Compostela, June 18–22, 2018

Computing perturbations in two-planetary three-body problem with masses varying non-isotropically at different rates

Mukhtar Minglibayev[1,2], **Alexander Prokopenya**[3], **Saule Shomshekova**[1,2]

The classical problem of three bodies of variable masses is considered in the case when two of the bodies are protoplanets and the masses vary non-isotropically at different rates. Reactive forces appearing due to the change of masses complicate the problem substantially and general solution of the equations of motion cannot be found in symbolic form. So the problem is analyzed in the framework of the perturbation theory in terms of the osculating elements of aperiodic motion on quasi-conic sections [1, 2]. An algorithm for symbolic computation of the perturbing function and its expansions in terms of eccentricities and inclinations is discussed in detail.

Keywords: Three-body problem, protoplanets, variable masses, perturbations, Mathematica

References

[1] M.ZH. MINGLIBAYEV, *Dynamics of Gravitating Bodies of Variable Masses and Sizes*. Lambert Academic Publ., 2012.

[2] M.ZH. MINGLIBAYEV, A.N. PROKOPENYA, G.M. MAYEMEROVA, ZH.U. IMANOVA, Three-body problem with variable masses that change anisotropically at different rates. *Mathematics in Computer Science* **11**, 383–391 (2017).

[1]al-Farabi Kazakh National University
al-Farabi av. 71, 050040, Almaty, Kazakhstan
minglibayev@gmail.com

[2]Fesenkov Astrophysical Institute
Observatoriya 23, 050020, Almaty, Kazakhstan
shomshekova.saule@gmail.com

[3]Department of Applied Informatics
Warsaw University of Life Sciences – SGGW
Nowoursynowska 166, 02-787, Warsaw, Poland
alexander_prokopenya@sggw.pl

Applications of Computer Algebra – ACA2018
Santiago de Compostela, June 18–22, 2018

Motion of two bodies coupled by a spring on a rough plane with variable coefficient of friction: simulation with Mathematica

Alexander N. Prokopenya[1]

Two bodies of the same mass m connected by a spring move along a straight line Ox of a horizontal plane which is smooth for $x < 0$ and is rough for $x \geq 0$. Initially both bodies are located in the domain $x < 0$ and have the same velocity $v_0 > 0$. Assume that at the initial instant of time $t = 0$ the spring is not deformed and the x-coordinates of the bodies are $x_1(0) = -l_0$, $x_2(0) = 0$, where l_0 is the length of non-deformed spring. The problem is to investigate the motion of the system when the second body enters the domain $x > 0$ and starts to move on a rough surface. In this case the second body is acted on by the dry friction force directed opposite to the velocity of the body (see [1, 2]). As the spring is compressed and exerts a force on each of the bodies, one can write the equations of motion in the form

$$\begin{aligned} \ddot{x}_2 &= -\mu g - \frac{k}{m}(x_2 - x_1 - l_0), \\ \ddot{x}_1 &= \frac{k}{m}(x_2 - x_1 - l_0), \end{aligned} \tag{1}$$

where μ is a friction factor, k is the spring constant, g is the gravity acceleration, and m is a mass of each body. It is assumed that only the second body moves on the rough semi-plane and its velocity $\dot{x}_2(t) > 0$. Solution to the system (1) can be found in symbolic form and application of the built-in Mathematica function *DSolve* (see [3]) gives

$$\begin{aligned} x_1(t) &= -l_0 + v_0 t - \frac{\mu g t^2}{4} + \frac{\mu m g}{4k}\left(1 - \cos\left(\sqrt{\frac{2k}{m}}t\right)\right), \\ x_2(t) &= v_0 t - \frac{\mu g t^2}{4} - \frac{\mu m g}{4k}\left(1 - \cos\left(\sqrt{\frac{2k}{m}}t\right)\right). \end{aligned} \tag{2}$$

Analysis of solution (2) shows that for some instant of time $t = t_1$ which is a root of the equation

$$v_0 - \frac{\mu g t_1}{2} = \frac{\mu g}{2}\sqrt{\frac{m}{2k}}\sin\left(\sqrt{\frac{2k}{m}}t_1\right), \tag{3}$$

velocity of the second body $\dot{x}_2(t_1)$ becomes equal to zero while $x_1(t_1) < 0$ and $\dot{x}_1(t_1) > 0$. If the condition $|x_2(t_1) - x_1(t_1) - l_0| < \mu m g/k$ is fulfilled the second body stops while the first one continues to move. Further motion of the system

depends on the parameters k, m, l_0, μ, v_0, and different scenarios may be realized. Doing necessary symbolic and numerical calculations, we show that if elastic properties of the spring are asymmetric and its constant for stretching is greater than its constant for compressing then there exist such values of the system parameters for which the bodies are reflected from the rough semi-plane. Investigation of this interesting phenomenon is a main aim of the present talk.

Keywords: Motion of coupled bodies, dry friction, simulation, Wolfram Mathematica

References

[1] BO N.J. PERSSON, *Sliding friction. Physical principles and applications*. Springer-Verlag, Berlin, Heidelberg, 2000.

[2] LE X. ANH, *Dynamics of mechanical systems with Coulomb friction*. Springer-Verlag, Berlin, Heidelberg, 2003.

[3] S. WOLFRAM, *An elementary introduction to the Wolfram Language*. Wolfram Media, Champaign, IL, USA, 2017.

[1]Department of Applied Informatics
Warsaw University of Life Sciences – SGGW
Nowoursynowska str. 166, 02-787 Warsaw, Poland
alexander_prokopenya@sggw.pl

Applications of Computer Algebra – ACA2018
Santiago de Compostela, June 18–22, 2018

A study of sensitivity of nonlinear oscillations of a CLD parallel circuit to parametrization of Esaki diode

Haiduke Sarafian[1]

Esaki diode, also known as, a tunneling diode [1] is a peculiar nonlinear electronic element possessing negative ohmic resistance. We consider a multi-mesh circuit composed of three elements: a charged capacitor (C), a self-inductor (L), and an Esaki diode (D). All three elements in the circuit are parallel. We parametrize the I-V characteristics of the diode and derive the circuit equation; this is a nonlinear differential equation. Applying a Computer Algebra System (CAS) specifically Mathematica [2] we solve the equation numerically conducive to a diode dependent parametric solution. The solution is oscillatory. In this note we investigate the sensitivity of the nonlinear oscillations as a function of these parameters. Particularly we establish the fact that for a set of parameters the tunneling diode becomes an ohmic resistor and the circuit equation simplifies to a classic CLR parallel circuit with linearly damped oscillations. Mathematica simulation assists visualizing the transition.

Keywords: Esaki Diode, Electrical Nonlinear Oscillations, Computer Algebra System, Mathematica

References

[1] *Leo Esaki diode*. https://en.wikipedia.org/wiki/Tunnel_diode

[2] *Mathematica^{TM} (2017) is symbolic computation software*, V11.2, Wolfram Research Inc.

[1]The Pennsylvania State University
University College
York, PA 17403
has2@psu.edu

Applications of Computer Algebra – ACA2018
Santiago de Compostela, June 18–22, 2018

3D Stress analysis of a loaded birefringent sphere by photoelastic experiment and finite elements method

Kamel Touahir[1], **Ali Bilek**[1], **Said Larbi**[1], **Said Djebali**[1] and **Philippe Bocher**[2]

This paper deals with a contact problem developed in a birefringent sphere loaded by a plan along its diameter. In mechanical systems, contacts between moving elements can give rise to high stresses that can cause damage. Several authors [1, 2, 3, 4, 5] have contributed to the understanding of contact problems. To improve the design and the durability, it is necessary to determine accurately the stress fields particularly in the neighborhood of the contact zones. The analyzed model consists of a birefringent deformable sphere loaded along its diameter by birefringent rigid plans. Stress fields are analyzed experimentally with plan polarized light and circularly polarized light; photoelastic fringes are used to calculate stresses. A finite elements analysis with Castem package allows calculating the stress fields. Comparison between the experimental solution and the finite element one shows good agreements.

Experimental analysis

The birefringent sphere is machined from a birefringent parallelepiped on a high speed numerically controlled machine. The model is then loaded inside an oven (figure 1left) at the stress freezing temperature (120^oC). A thermal cycle is used to freeze stresses within the volume of the model. The model is then mechanically sliced in a high speed rotating machine to prevent residual stresses. The birefringent

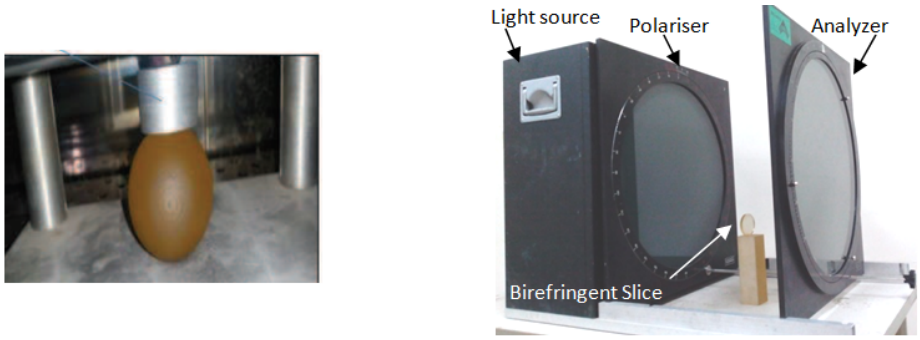

Figure 1: Sphere inside the oven (left), a slice analyzed in a polariscope (right)

slice is then positioned in the light path of a polariscope (figure 1 right) to obtain the photoelastic fringes. The light intensity after the analyzer is given by Eq. (1).

The terms $\sin^2 2\alpha$ and $\sin^2 \varphi/2$ give respectively the isoclinic fringe pattern and the isochromatic fringe pattern where α and φ are respectively the isoclinic parameter and the isochromatic parameter [6].

$$I = a^2 \sin^2 2\alpha \sin^2 \varphi/2 \tag{1}$$

The experimental isochromatic fringes are used to determine the values of the principal stresses difference in the model by using the well known Eq. (2).

$$\sigma_1 - \sigma_2 = \frac{Nf}{e} \tag{2}$$

Where N is the fringe order, f is the photoelastic fringe value, and e is the model thickness. The values of the fringe order N are determined experimentally.
A $10mm$ thickness slice along the load direction (figure 2) is analyzed with plane polarized light on a regular polariscope. One can see clearly the isochromatics and the isoclinics developed on the model particularly in the neighborhood of the contact zones where stresses are higher (zone of maximum shear stress).

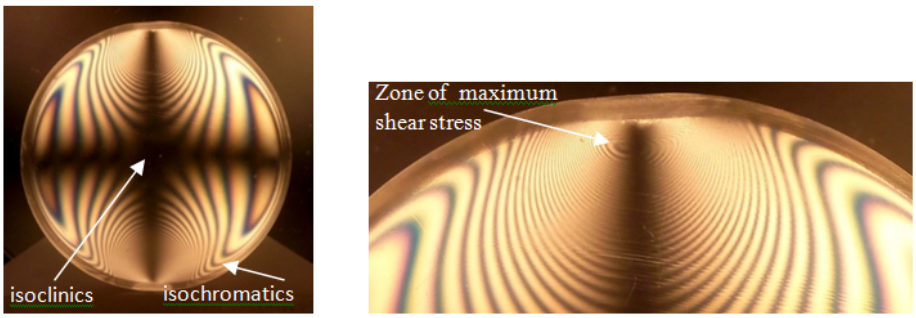

Figure 2: Photoelastic fringes obtained with plan polarized light

Numerical analysis

A finite element analysis is used to determine the stress fields developed in the models particularly in the neighborhood of the contact zones; a program developed under *castem package* allowed us to obtain stress values as well as numerical photoelastic fringes that can be compared to the experimental photoelastic fringes. The analysis is performed in the elastic domain. The meshing is refined in the neighborhood of the contact zone for a better simulation (figure 3).
The isoclinic fringe pattern is calculated with eq. (3) where α is the isoclinic parameter [6]. Once α is obtained the value of $\sin^2 2\alpha$ gives directly the isoclinic fringe pattern.

$$\alpha = \arctan(2\tau_{xy}/(\sigma_x - \sigma_y)) \tag{3}$$

The simulated isochromatic fringe patterns are obtained with eq. (4). The different values of $\sin^2 \varphi/2$ give then easily the numerical isochromatic fringes.

$$\varphi = \frac{2\pi e}{f}\sqrt{(\sigma_x - \sigma_y)^2 + 4\tau_{xy}^2} \tag{4}$$

The graph of variation of the principal stresses difference (Fig. 3) is obtained along the vertical axis. Stresses increase up to approximately $0.6MPa$ and then decrease as we move away from the contact zone. We can see relatively good agreement between the two solutions.

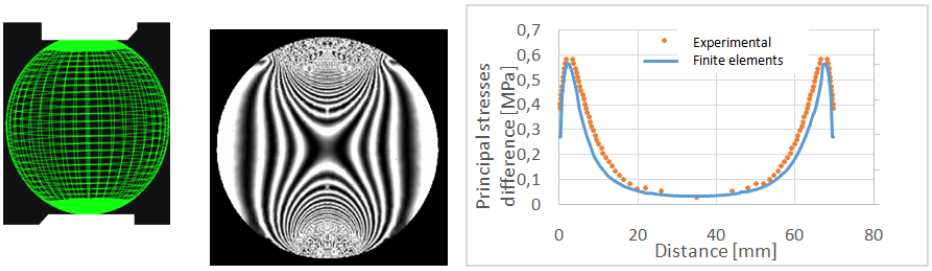

Figure 3: Model meshing and isochromatic fringes for a slice along the load direction

Keywords: photoelasticity, birefringent, isochromatic, isoclinic, contact, stress

References

[1] ABODOL RASOUL SOHOULI, ALI MAOZEMI GOUDARZI, REZA AKBARI ALASHTI, Finite Element Analysis of Elastic-Plastic Contact MechanicConsidering the Effect of Contact Geometry and Material Propertie. *Journal of Surface Engineered Materials and Advanced Technology* **1**(3), 125–129 (2011).

[2] J. A. GERMANEAU, F. PEYRUSEIGT, S. MISTOU, P. DOUMALIN AND J.C. DUPRÉ, Experimental study of stress repartition in aeronautical spherical plain bearing by 3D photoelasticity : validation of a numerical model. In *5th BSSM International Conference on Advances in Experimental Mechanics*, University of Manchester, UK,Sept. 2007.

[3] L. KOGUT & I. ETSION, Elastic-Plastic contact analysis of a sphere and a rigid flat. *Journal of Applied Mechanics* **69**(5), 657–662 (2002).

[4] BUDIMIR MIJOVICAND MUSTAPHA DZOCLO, Numerical contact of a Hertz contact between two elastic solids. *Engineering Modeling* **13**(3-4), 111–117 (2000).

[5] RABAH HACIANE, ALI BILEK, SAID LARBI, SAID DJEBALI, Photoelastic and numerical analysis of a sphere/plan contact problem. *Procedia Engineering* **114**, 277–182 (2015).

[6] J. W DALLY AND F. W. RILEY, *Experimental stress analysis*. McGraw-Hill, Inc, 1991.

[1]LMSE Laboratory, Mechanical Engineering Department
Mouloud Mammeri University of Tizi-Ouzou
P.O. Box17 RP, 15000 Tizi Ouzou, Algeria
alibilek2000@yahoo.fr

[2]Mechanical Engineering Department
Ecole de Technologie Supérieure
1100 Rue Notre-Dame, Montreal, H3C 1K3, Canada

Applications of Computer Algebra – ACA2018
Santiago de Compostela, June 18–22, 2018

Visualization of Planetary Motions Using KeTCindy

Satoshi Yamashita[1], **Kiyoshi Kitahara**[2], **Shuhei Miyake**[3], **Setsuo Takato**[4]

KeTCindy, a plug-in for a dynamic geometry software Cinderella, facilitates the creation of precise and beautiful drawings of 2D/3D graphics and their input into a LaTeX document. Moreover, KeTCindy can call other mathematical software to run a program and bring back the results. For a task of visualizing planetary motion, the authors call the computer algebra software Maxima to execute mathematical expression processing. Then they create PDF slides that portray planetary motion precisely based on the result[1].

About planetary motion, J. Kepler published the following three laws in 1619, having found them by analyzing the astronomical observations of T. Brahe.

1. The orbit of a planet is an ellipse with the Sun at one of the two focuses. Letting r be the distance from the Sun to the planet and letting θ be the angle to the planet's current position from its closest approach, as seen from the Sun, then the polar coordinates $(r,\ \theta)$ satisfy the polar equation of the ellipse:

$$r = \frac{l}{1 + \varepsilon \cos\theta}, \tag{1}$$

where l is the semi-latus rectum and ε is the eccentricity of the ellipse.

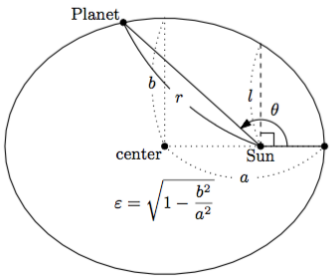

Figure 1: Elliptical orbit of the planet.

2. A line segment joining a planet and the Sun sweeps out equal areas during equal intervals of time. Because the planetary area velocity $\frac{dS}{dt}$ is constant, we obtain the following formula.

$$\frac{dS}{dt} = \frac{1}{2} r^2 \frac{d\theta}{dt} = \kappa \ \ (\text{Kepler}'\text{s constant}) \tag{2}$$

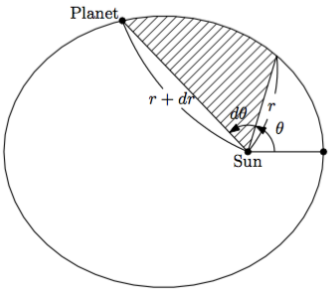

Figure 2: Planetary swept area.

3. The square of the orbital period of a planet is proportional to the cube of the semi-major axis of its orbit. Letting T be the orbital period and letting a the elliptical semi-major axis, then T and a satisfy the following condition.

$$\frac{T^2}{a^3} = C \ \ (\text{constant}) \tag{3}$$

In 1687, I. Newton derived Kepler's laws from the law of universal gravitation in his book "The Principia"[2].

Using KeTCindy, the authors calculate the planetary swept area as

$$2\kappa t = \int_0^t r^2 \frac{d\theta}{dt}\, dt = \int_0^t \frac{l^2}{(1+\varepsilon\, \cos\theta)^2}\, d\theta \tag{4}$$

and the planetary velocity vector

$$\frac{dx}{dt} = 2\kappa \left(\frac{\varepsilon \sin\theta \cos\theta}{l} - \frac{\sin\theta}{r} \right), \frac{dy}{dt} = 2\kappa \left(\frac{\varepsilon \sin^2\theta}{l} + \frac{\cos\theta}{r} \right) \tag{5}$$

and planetary acceleration vector, respectively, from Kepler's first law (1). Subsequently, they exhibit the calculated planetary motion so that the planetary area velocity is constant.

Keywords: Orbits of planets, Cinderella, Maxima, TeX, KeTCindy

References

[1] S. YAMASHITA; S. KOBAYASHI; H. MAKISHITA; S. TAKATO, PDF Slide Teaching Materials Created Using KeTCindy. In *Computer Science and Its Applications – ICCSA2017*, O. Gervasi et al. (eds.), pp.285–300, Springer, Italy, 2017.

[2] I. BERNARD; A. WHITMAN, *Isaac Newton, The Principia – Mathematical Principles of Natural Philosophy*. University of California Press, London, 1999.

[1]Department of Natural Science,
National Institute of Technology, Kisarazu College
2-11-1, Kiyomidai-Higashi, Kisarazu, 292-0041, Japan
yamasita@kisarazu.ac.jp

[2]Division of Liberal Arts
Kogakuin University
2665-1 Nakano, Hachioji, Tokyo 192-0015, Japan
kitahara@cc.kogakuin.ac.jp

[3]Department of Informatics, Faculty of Informatics,
Tokyo University of Information Sciences
4-1, Onari-dai, Wakaba-ku, Chiba, 265-8501, Japan
miyake.shuhei@gmail.com

[4]Department of Science,
Toho University
2-2-1, Miyama, Funabashi, 274-8510, Japan
takato@phar.toho-u.ac.jp

Applications of Computer Algebra – ACA2018
Santiago de Compostela, June 18–22, 2018

Fluid/Particles Flow Simulation by Finite Volume Method -Hybrid Approach-

Salah ZOUAOUI[1], **Hassane DJEBOURI**[1], **Ali BILEK**[1] and **Kamal MOHAMMEDI**[2]

We present here a numerical method to compute the motion of rigid particles in fluid flow with a non-elastic impact law. Many methods have been proposed recently and different strategies have been used to compute such flows [1]. Our motivation is the handling of the non-overlapping constraint in fluid-particle direct simulations [2, 3]. Each particle is treated individually and the Navier-Stokes equations are solved for the moving fluid by Fluent code which is based on the Finite volume method. The contact-handling algorithm is based on the projection of the velocity field of the rigid particles over the velocity field of the fluid flow. The method consists of imposing a constraint on the velocity field of the particles, as a guarantee that at each time step the calculated particle velocity field belongs to an eligible velocity field of the fluid. In this case study, an Uzawa algorithm has been applied [4].

Keywords: Simulation, Flow, Particles, Contact, Uzawa, Fluent

Contact Handling Procedure

Let us detail the method in the case of spherical particles: we denote by $\mathbf{X}^n := (\mathrm{x}_\mathrm{i}^\mathrm{n})_{i=1,.....,N}$ the position of N particles (more precisely, the position of their gravity centre) at time t_n, by $\hat{\mathbf{V}}^n = (\hat{\mathrm{v}}_i)_{i=1,.....,N}$ the a priori translational velocity, by $\hat{\Omega}^n = (\hat{\omega}_i)_{i=1,.....,N}$ the a priori rotational velocity. As stated before, the a priori updated position of the particles, defined as:

$$\mathbf{X}^{n+1} = \mathbf{X}^n + \Delta t \hat{\mathbf{V}}^n + \frac{1}{2}\gamma^n \triangle t^2 \tag{1}$$

where γ the acceleration, calculated from the Newton's second law. Equation 1 may lead to non-admissible configuration, in the sense that the particles overlap. To avoid this, we project the velocities onto the following set:

$$K(X^n) = \{\mathrm{V} \in \mathbb{R}^{2N}, D_{ij}(\mathrm{X}^n) + \Delta t \mathrm{G}_{ij}(\mathrm{X}^n).\mathrm{V} + \frac{1}{2}\gamma^n \triangle t^2 \geqslant 0, \forall i < j\} \tag{2}$$

where D_{ij} is the distance between every two particles given as:

$$D_{ij}(\mathrm{X}^n) = \|\mathrm{x}_i^n - \mathrm{x}_j^n\| - (R_i - R_j) \tag{3}$$

At each time step, $\mathrm{V} \in \mathbb{R}^{2N}$ is an admissible vector if the particles with velocity $\{\mathrm{V}$ do not overlap at the next time step:

$$E(X^n) = \{\mathrm{V} \in \mathbb{R}^{2N}, D_{ij}(\mathrm{X}^n + \Delta t \mathrm{V}^n + \frac{1}{2}\gamma^n \triangle t^2) \geqslant 0, \forall i < j\} \tag{4}$$

We not that equation 2 is the linearized form of equation 4 and, furthermore, it can be shown that $K(X^n) \subset E(X^n)$. It means in particular that particles with admissible velocities at time t_n do not overlap at time t_{n+1}.
The constrained problem is formulated as a saddle-point problem, by using the introduction of Lagrange multipliers:

$$\begin{cases} Find(\mathrm{V}^n, \Lambda^n) \in \mathbb{R}^{2N} \times \mathbb{R}_+^{N(N-1)/2} \quad suchthat \\ \mathcal{J}(\mathrm{V}^n, \lambda) \leqslant \mathcal{J}(\mathrm{V}^n, \Lambda^n) \leqslant \mathcal{J}(\mathrm{V}, \Lambda^n), \quad \forall (\mathrm{V}^n, \lambda) \in \mathbb{R}^{2N} \times \mathbb{R}_+^{N(N-1)/2} \end{cases} \tag{5}$$

with the following functional:

$$\mathcal{J}(\mathrm{V}, \lambda) = \frac{1}{2} \mid \mathrm{V} - \hat{\mathbf{V}}^n \mid^2 - \sum_{1 \leqslant i \leqslant j \leqslant N} \lambda_{ij}(D_{ij}(\mathrm{X}^n) + \Delta t \mathrm{G}_{ij}(\mathrm{X}^n).\mathrm{V}) + \frac{1}{2}\gamma^n \triangle t^2 \tag{6}$$

Where $\mathrm{G}_{ij}(\mathrm{X}^n) \in \mathbb{R}^{2N}$ is the gradient of distance D_{ij}. The number of Lagrange multipliers (λ_{ij}) corresponds to the number of possible contacts. This problem is solved by an Uzawa algorithm.

Falling of 50 particles of different sizes on a plane

The computer implementation of the contact Handling algorithm allows us to simulate the falling of 50 particles of different sizes on a plane (figure1). This allows us to highlight the particle/particle and particle/wall contact.

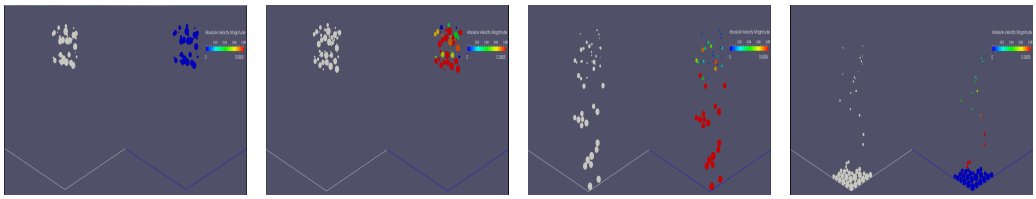

$t = 0.0s$ $t = 0.10s$ $t = 0.20s$ $t = 0.80s$

Figure 1: Fall down of 50 particles of different sizes on a plane

Simulation of the water flow inside a pipe with obstacles

The incompressible Navier-Stokes equations are written in the following form.

$$\begin{cases} \rho_f \dfrac{Du}{Dt} - \mu \Delta u + \nabla p = f_{\ \Omega \backslash \overline{B}} & \text{dans } \Omega \\ \nabla . u = 0 & \text{dans } \Omega \\ u = 0 & \text{sur } \partial\Omega \end{cases} \tag{7}$$

where ρ_{f} denotes the density of the fluid, $\mathrm{u}(u_1, u_2)$ the velocity of fluid, σ the the stress tensor and $\mathbf{f}_{\mathrm{f}} = \rho_{\mathrm{f}} g e_y$ is the external force exerted on the fluid (gravity forces). We used a Fluent commercial code to solve equation 7.

Fluid-Particles Simulation

In this test case, we simulated the transport of solid particles in a pipe with obstacles (figure 2). To take into account the solid particles we integrated, in the code of contact management, the equations of the solid dynamics by considering all the forces acting on a particle in a fluid flow. On the other hand, for the numerical resolution of the Navier-Stokes equations, we resorted to the use of a Fluent commercial code which is based on the finite volume method.

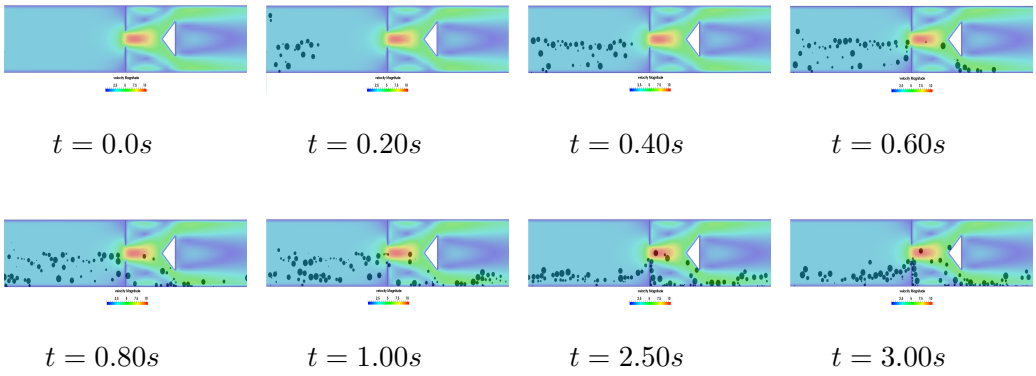

Figure 2: Injection of solid particles: Configuration at different time steps

References

[1] ZOUAOUI, S., DJEBOURI, H., BILEK, A. ET AL., Modelling and Simulation of Solid Particle Sedimentation in an Incompressible Newtonian Fluid. *Math.Comput.Sci.* **11**(3-4), 527–539 (2017).

[2] MAURY, B., A time-stepping scheme for inelastic collisions. *Numerische Mathematik* **102**(4), 649—679 (2006).

[3] ALINE LEFEBVRE., Fluid-particle simulations with freefem++. *InESAIM: Proceedings* **18**(4), 120—132 (2007).

[4] BANK, R.,WELFERT, B., AND YSERENTANT, H.,A class of iterative methods for solving saddle point problems. *Numerische Mathematik* **56**(7), 645–666. (1989).

[1]LMSE Laboratory
Mechanical Engineering Department
Mouloud Mammeri University of Tizi-Ouzou
P.O. Box17 RP, 15000 Tizi Ouzou, Algeria
zouaoui_salah2003@yahoo.fr; zouaouisalah@ummto.dz

[2]Unité de Recherche Matériaux, Procédés et Environnement (URMPE)
MESOnexusteam
Université M'hamed Bougara Boumerdès
Algérie 35000
mohammedik@yahoo.com